Increased Trimethylamine N-oxide Contributes to Metabolic dysfunction in a Rat Model of PCOS and Decreases Mitochondrial function

Huang Jiayu
Wuhan Union Hospital
Liu Jiaying
Wuhan Union Hospital
Zhang Hanke
Wuhan Union Hospital
Li Yajie
Wuhan Union Hospital
Minuo Yin
Department of Obstetrics and gynecology, Wuhan Union Hospital. Tongji Medical College, Huazhong University of Science and Technology, Wuhan, China
Jing Guo
Chongqing Health Center for Women and Children
Chong Li
Chongqing Health Center for Women and Children
Yinhua Qin
Chongqing Health Center for Women and Children
Jingyu Li
Chongqing Health Center for Women and Children
Ying Gao (gaoyingpro@163.com)
Wuhan Union Hospital

Research

Keywords: Polycystic ovarian syndrome, trimethylamine N-oxide, in vitro maturation, mitochondrial function

Posted Date: December 10th, 2020

DOI: https://doi.org/10.21203/rs.3.rs-122457/v1

Abstract

Polycystic ovarian syndrome (PCOS) is a common endocrine disease in adolescents and women of childbearing age, also a common cause of female infertility. In recent years, studies have found that the occurrence of PCOS is related to changes in the intestinal flora. Trimethylamine N-oxide (TMAO) is an organic compound produced by intestinal microorganisms. However, the relationship between TMAO and PCOS remain mostly unexplored. The effects of TMAO on PCOS were assessed in vitro and in vivo. In a PCOS rat model, plasma TMAO, hormone and PI3K signaling levels were examined. In the process of in vitro maturation (IVM), immunofluorescence and confocal microscopy were used to detect the influence of adding different TMAO concentrations to the culture medium on oocytes. The fasting insulin (FINS), HOMA-IR, luteinizing hormone (LH), LH/follicle-stimulating hormone (FSH) and plasma TMAO levels of the PCOS rat group were significantly higher than those of the control group. Treatment with the TMAO inhibitor 3,3-dimethyl-1-butanol (DMB) alleviated metabolic disorder in PCOS rats. In PCOS rats, DMB improved the PI3K/Akt-related signaling pathway compared to no treatment. In IVM, the mitochondria of oocytes in the TMAO groups were aggregated and distributed, and mitochondrial membrane potential and ATP content were decreased. Apoptosis was more severe in the TMAO group than in the control group. TMAO worsened metabolic dysfunction in a rat model of PCOS and decreased the mitochondrial function of oocytes in the process of IVM.

1. Introduction

Polycystic ovarian syndrome (PCOS) is a common endocrine disease in adolescents and women of childbearing age and a common cause of female infertility[1, 2]. Common clinical manifestations include menstrual disorder, infrequent ovulation, chronic anovulation, hirsutism, hyperandrogenism (HA), insulin resistance (IR) and polycystic ovarian changes[1, 3, 4]. PCOS is usually diagnosed according to the Rotterdam criteria, given the presence of at least two of three criteria, clinical or laboratory HA, ovulatory dysfunction or polycystic ovaries on ultrasound[5]. Long-term complications include type 2 diabetes mellitus (T2DM), hypertension, cardiovascular disease (CVD), endometrial cancer, etc., and the health and quality of life of women suffering from PCOS are seriously threatened[6, 7]. With alterations in luteinizing hormone (LH), follicle-stimulating hormone (FSH), anti-Müllerian hormone (AMH), insulin-like growth factor (IGF) and androgen levels, PCOS patients may suffer from failure of selection of the dominant follicle and ovulation as well as an abnormal ovarian cycle[8]

The intestinal flora is considered to be the “second brain” or “second genome” of humans. It is one of the most complex microbial communities and includes more than 1000 bacteria and participates in the coding of more than 3 million nonredundant genes. This number is approximately equal to the total number of host human cells[9, 10], and through long-term coexistence, low-level exposure of the host to metabolic and decay products affects the host's important physiological functions, such as metabolism, immunity and signal transduction pathways[11]. The intestinal flora and the human body are interdependent and form a state of dynamic balance that can change with age, diet, and environmental changes. When the gene expression level of the gut microbiota is relatively low or microbial diversity is

reduced, the metabolic health of the host may be impaired[11]. Recent studies have found that the occurrence of PCOS is related to changes in the intestinal flora[12–14]. Studying changes in the intestinal flora and its metabolites related to PCOS may provide new ideas for the pathogenesis and therapeutic targets of PCOS.

Trimethylamine N-oxide (TMAO) is an organic compound produced by intestinal microorganisms[15]. The phosphatidylcholine, choline and carnitine in the diet are metabolized to trimethylamine (TMA) under the action of certain intestinal microorganisms. After being absorbed into the blood, TMA enters the liver through the portal circulation, where it is found in flavin monooxidase (FMO), and quickly transformed into TMAO[16]. Studies have found that the occurrence of T2DM is related to an increase in the plasma TMAO concentration[17]. Oellgaard et al.[18] found that an increase in plasma insulin levels caused by IR increased FMO3 activity and further increased TMAO serum levels. Studies have also shown that in atherosclerosis, TMAO upregulates scavenger receptors in macrophages and promotes the accumulation of cholesterol in macrophages and the formation of foam cells, thereby promoting vascular plaque through the MAPK and NF-κB pathways and the inflammatory response[19].

Another study found that TMAO enhances platelet reactivity and increases the risk of thrombosis and has an adverse effect on cardiovascular function[20, 21]. TMAO is involved in metabolic or inflammatory diseases such as CVD, T2DM and thrombosis. According to our latest research, plasma TMAO concentrations are high in patients suffering from PCOS without hyperandrogenism[22]. Nagy et al.[23] found that TMAO is present in human follicular fluid and a negative predictor of embryo quality. To date, however, no studies have directly examined the role of TMAO in mediating metabolic dysfunction in PCOS. Here, we tested the hypothesis that elevated TMAO contributes to metabolic dysfunction in a rat model of PCOS and reduces oocyte quality.

2. Materials And Methods

2.1. Ethics statement

All animal experiments were carried out in accordance with the principles and guidelines for the use of laboratory animals and approved by the Institutional Animal Care and Use Committee of Wuhan Union Hospital, Tongji medical college, HUST.

2.2. Establishment of rat models

A total of 24 female Sprague–Dawley (SD) rats of specific pathogen-free (SPF) degree were purchased from Beijing Charles River Co., Ltd. The rats (age, 9 weeks; weight, 250–300 g) were randomly arranged to the control group (n = 8), the PCOS group (n = 8) or the DMB group (n = 8). The PCOS and DMB groups were given insulin plus hCG to induce a combination of hyperinsulinemia and hyperandrogenism. The control group was treated with an equal volume of saline. The doses and treatment protocols for insulin and hCG were described in studies by Poretsky[24] and Zhang[25, 26]. Briefly, insulin was started at 0.5 IU/day and gradually increased to 6.0 IU/day between the first day and the 22nd day to induce

hyperinsulinemia and IR, and 3.0 IU/day hCG was given to induce hyperandrogenism. Animals were treated with twice daily subcutaneous injections until the end of the experiment. Rats in the DMB group received 1.0% 3,3-dimethyl-1-butanol (DMB, an inhibitor of trimethylamine formation, 8 weeks after DMB treatment, when circulating TMAO levels were reduced in rats) for 8 weeks in drinking water. Vaginal smears and Pap stains were performed daily since the beginning of modeling to observe changes in cytology.

2.3. Collection and storage of specimens

After 8 weeks, all rats were fasted for 12 hours for measurements of fasting blood glucose (FBG) and fasting insulin (FINS). FBG was tested with a blood glucose meter (F. Hoffmann-La Roche Ltd., Switzerland), and enzyme-linked immunosorbent assay (ELISA) kits were used for the determination of FINS (RayBiotech Company, USA). Rats were sacrificed on the second day after the end of the FBG and FINS experiments. Blood samples were collected from the abdominal aorta, separated from the serum (blood was collected in a centrifuge tube, let stand at room temperature for 1 hour for coagulation and stratification, and centrifuged at 3000 rpm for 10 minutes at room temperature, and the supernatant was removed and transferred to a clean centrifuge tube and stored at -80 °C) and plasma (plasma was centrifuged in a low-temperature centrifuge at 4 °C and 3000 rpm for 10 minutes, approximately 1 ml of the upper layer of transparent liquid was absorbed, the tightness was reviewed, and the sample was placed in a box and stored in an ultra-low-temperature refrigerator at -80 °C) to be tested. The right ovary was quickly frozen in liquid nitrogen and stored at -80 °C for later analyses, and the left ovary was fixed using 10% neutral-buffered formaldehyde for further histopathological examinations.

2.4. Determination of plasma TMAO

The plasma TMAO level was detected by Liquid chromatography coupled with triple-quadrupole mass spectrometry (ACQUITY UPLC H-Class / Xevo G2 TQ-XS MS/MS) for quantitative detection (Metabo-Profile, Shanghai, P. R. China)[27].

2.5. Determination of sex hormones

ELISA kits were used for the determination of testosterone (R&D Systems, USA), FSH (Enzo Company, USA), LH(Enzo Company, USA), and estrogen (R&D Systems, USA). Then, the LH/FSH ratio and HOMA-IR index were calculated as follows: [HOMA-IR = FPG (mmol/L) × FINS (mIU/L) / 22.5].

2.6. Western blot analysis

Protein was isolated from frozen ovarian tissues. Protein concentration was determined using the Bradford method. The protein samples (30 μg per lane) were separated by 10% SDS-PAGE, transferred to a polyvinylidene fluoride (PVDF) membrane (Millipore, USA), and then blocked with 5% nonfat milk at room temperature for 1 h. The membrane was incubated overnight at 4 °C with primary antibodies, including those against PI3K (Cell Signaling Technology, USA), phospho-Akt (Cell Signaling Technology, USA), Akt (Cell Signaling Technology, USA), IRS (Cell Signaling Technology, USA), and β-actin (GeneTex, USA). After incubation with goat anti-rabbit IgG H&L (HRP) (Abcam, USA) for 1 h at room temperature, the

cells were detected with a BioSpectrum 600 Imaging System (USA). The band density was determined with ImageJ software (National Institutes of Health, Bethesda, MD, USA).

2.7. Oocyte collection of mice and in vitro maturation

For in vitro maturation (IVM), ovaries were collected from six-week-old specific pathogen free (SPF) female mice (20–25 g body weight), purchased from the Beijing Vital River Experimental Animals Centre (Beijing, China). They received 10 IU of pregnant mare serum gonadotropin (PMSG) (Ningbo Second Hormone Factory, Zhejiang, China). Forty-eight hours later, mice ovaries were excised, and the COCs were isolated from the ovary and put into M16 medium. The oocytes were applied in the following experiments.

During this experiment, TMAO (Sigma, St. Louis, MO, USA) was dissolved and diluted with M16 medium to a final concentration of 10 μM and 100 μM respectively.

2.8. Immunofluorescent and confocal microscopy

All experiments were performed three times and observed under a laser-scanning confocal fluorescent microscope (Leica, German). Mito-Tracker Red CMXRos and Mitochondrial membrane potential assay kit with JC-1 (Beyotime, China) were used to label the mitochondria and measure the mitochondrial membrane potential (Δψm) of oocytes. Carboxy-H2DCFDA (general oxidative stress indicator) (Thermo, USA) was applied to determine the ROS level. Annexin-V staining kit (Thermo, USA) was used to evaluate the apoptosis of the oocytes. Enhanced ATP assay kit (Beyotime, China) was applied in the detection of semiquantitative ATP levels.

For the quantification of fluorescence intensity, the images from both control and treated oocytes were acquired by performing the same immunostaining procedure and setting up the same parameters of confocal microscope. Then ImageJ software was used to measure the fluorescence intensity of region of interest in the images.

2.9.Statistical analysis

All statistical analyses were performed using STATA (Chicago, IL, USA), ImageJ and GraphPad Prism 6 (GraphPad Software Inc., San Diego, CA, USA). The data are expressed as means ± SDs. A $P < 0.05$ was considered significant.

3. Results

3.1. Changes in rat body weight and estrus cycle

The weight gain of rats in the PCOS group and DMB group after modeling was lower than that of rats in the control group, and the difference was statistically significant (Table 1). After modeling, vaginal secretion smears showed that all rats in the PCOS group had estrous cycle disturbances and lost

periodicity, while 5 of 8 in the DMB group had estrous cycle disturbances, and the other 3 rats maintained normal estrus cycles (Fig. 1).

Table 1
Changes in body weight of rats before and after treatment

	Control	PCOS	DMB
Start Weight (g)	297.4 ± 18.2	298.3 ± 16.5	296.5 ± 13.5
End Weight (g)	353.0 ± 19.9	347.9 ± 22.0	331.6 ± 17.3
Gain Weigh (g)	55.7 ± 8.08	49.5 ± 10.1	35.5 ± 11.5^{ab}

Data are presented as the mean ± SD. $^{a}P < 0.05$ versus Control group, $^{b}P < 0.05$ versus PCOS group

3.2. Changes in ovarian structure

HE staining results showed, the ovaries of the control group and DMB group rats were generally morphologically regular and the presence of various levels of follicles, and the granular cells were arranged neatly and completely. In PCOS group, the ovaries showed polycystic changes, multiple cystic expanded follicles, some oocytes were absent, some atretic follicles were seen, granulosa cell layer decreased, and stromal cells proliferated. (Fig. 2)

3.3. FBG, FINS, hormones and TMAO

FINS test results showed that the serum insulin level of rats in the PCOS group and DMB group was higher than that of rats in the control group, but the insulin level of rats in the DMB group was significantly lower than that of rats in the PCOS group. The HOMA-IR value was calculated according to the FBG level and FINS level. The rats in the PCOS group had impaired glucose tolerance and decreased insulin sensitivity, indicating that this group of rats had IR, while the HOMA-IR value did not differ between the DMB group and the control group. (Table 2)

Table 2
FBG, hormones and TMAO of rats

	Control	PCOS	DMB
FBG(mmol/L)	4.38 ± 0.32	4.14 ± 0.32	3.89 ± 0.14[ab]
FINS(μIU/ml)	14.95 ± 1.87	22.01 ± 4.84[a]	17.97 ± 2.04[a]
HOMA-IR	2.91 ± 0.45	4.02 ± 0.74[a]	3.10 ± 0.33[b]
FSH(mIU/ml)	1.99 ± 0.67	2.02 ± 0.69	1.95 ± 0.37
LH(mIU/ml)	2.03 ± 0.37	2.56 ± 0.41[a]	1.84 ± 0.99[b]
LH/FSH	1.14 ± 0.44	1.43 ± 0.58[a]	0.94 ± 0.44[b]
TMAO(μmol/L)	0.72 ± 0.25	1.15 ± 0.16[a]	0.69 ± 0.19[b]

Data are presented as the mean ± SD. [a]P < 0.05 versus Control group, [b]P < 0.05 versus PCOS group

3.4. AKT phosphorylation level and IR level in rat ovarian tissue

As shown in Fig. 3, Western blot results showed that the protein expression of PI3K in the ovaries of rats in the DMB group was significantly higher than that of rats in the PCOS group, while the PCOS group had obviously reduced p-Akt/Akt levels compared with the control group. Although the PCOS group had a higher level of IRS protein expression, the difference was not significant.

3.5. Oocyte maturation

COCs were cultured in M16 medium containing two concentrations of TMAO (10 μM and 100 μM) or without TMAO (control group) for 12–14 hours. We observed that the number of metaphase II oocytes was significantly lower in medium supplemented with 10 μM TMAO and 100 μM TMAO than in the control medium. However, in M16 medium supplemented with TMAO, the rate of nuclear maturation was not significantly different compared to that of the control medium. The effects of TMAO on spindle/chromosome defects were not significantly different (Fig. 4).

3.6. Content and distribution of mitochondria in oocytes

Our results (Fig. 5) showed that the relative fluorescence intensity of mature oocytes in the TMAO-10 μM and TMAO-100 μM experimental groups was significantly weaker than that of those in the control group (P < 0.0001). The mitochondria of oocytes in the control group were evenly distributed, and the mitochondria of oocytes in the TMAO group were aggregated and distributed, indicating that when the

concentration of TMAO in the culture medium reached 10 μmol/L, the content of mitochondria in oocytes decreased, and the distribution appeared abnormal.

3.7. ROS in oocytes

H2DCFDA staining was carried out to determine the ROS levels in oocytes. The results indicated that the ROS level in oocytes was not significantly higher in the groups treated with 10 μM TMAO and 100 μM TMAO than in the control group (Fig. 6).

3.8. mitochondrial membrane potential in oocytes

JC-1 was used as a fluorescent probe to quickly and sensitively detect changes in the mitochondrial membrane potential (ΔΨm) of oocytes. When the mitochondrial membrane potential decreased, JC-1 changed from red fluorescence to green fluorescence. As shown in Fig. 7, the average ratio of red-green fluorescence in mouse oocytes cultured in vitro for 14 h in medium supplemented with TMAO was significantly lower than that of oocytes cultured in control medium. Statistical analysis showed that the mitochondrial membrane potential was lower in the TMAO-100 μM and control groups than in the TMAO-10 μM group. These results indicate that TMAO reduces the mitochondrial membrane potential of oocytes and impairs mitochondrial function.

3.9. ATP in oocytes

We collected 30 MII oocytes from each of the 3 groups, used an enhanced ATP detection kit to measure the chemiluminescence intensity of ATP standard products to obtain a standard curve (R^2 = 0.9946), and calculated the relative control of each sample according to the chemiluminescence intensity of each sample. The ATP content of oocytes in the TMAO-100 μM group was significantly lower than that in the control and TMAO-10 μM groups. (Fig. 8)

3.10. Apoptosis

Green fluorescent circles on the oocyte membrane were clearly observed in the oocytes of the experimental groups, while those in the oocytes of the control group were relatively weak. Statistical analysis showed that the relative fluorescence intensity of the experimental group was much higher than that of the control group, and as the concentration of TMAO increased, the fluorescence intensity increased. (Fig. 9)

4. Discussion

PCOS is a common metabolic disorder in women of childbearing age, and investigating the mechanisms of PCOS is of great significance. In the PCOS rat experiment, the FINS, HOMA-IR, LH, LH/FSH and plasma TMAO levels of the PCOS group were significantly higher than those of the control group. Treatment with the TMAO inhibitor DMB alleviated metabolic disorder in PCOS. Insulin can activate the tyrosine kinase

domain of the insulin receptor, which phosphorylates the phosphotyrosine residues on the insulin receptor substrate, activates the PI3K/Akt signaling pathway, and increases the uptake of glucose by cells. Our study found that the PI3K/Akt signaling pathway was inhibited in PCOS rats and that the addition of 1% DMB to the drinking water improved the PI3K/Akt-related signaling pathway.

A large number of studies have confirmed that mitochondria, as an important part of cell metabolism, are related to obesity, metabolic syndrome, T2DM, and CVDs[28–30]. The latest research shows that a certain concentration of TMAO can affect mitochondrial function in atherosclerosis. TMAO can cause the overexpression of succinate dehydrogenase complex subunit B (SDHB) in human umbilical vein endothelial cells (HUVECs), resulting in damage to the mitochondria and increased levels of ROS, which promote the apoptosis of vascular endothelial cells and thereby the development of atherosclerotic lesions[31]. Mitochondrial dysfunction may be related to the IR associated with PCOS (i.e., when mitochondrial function declines, the oxidation reaction in the cell is weakened, leading to lipid accumulation and thereby inhibiting insulin signaling[32] and further aggravating the symptoms of PCOS patients). In this study, we found that the intestinal flora product TMAO reduced the MII rate of mouse oocyte maturation in vitro, reduced oocyte mitochondrial content and abnormal distribution, reduced mitochondrial membrane potential, reduced ATP content, and accelerated the early apoptosis of oocytes. A decrease in mitochondria in oocytes leads to a decrease in ATP produced by aerobic respiration, and ATP provides the energy required for cellular activities. Oocytes need a sufficient energy supply during maturation, so TMAO can reduce the number of and damage to mitochondria, and its function directly affects the quality of oocytes.

In recent years, more attention has been given to the intestinal flora, as a mountain of new evidence has shown that the microbiota plays an influential role in human health and disease[19, 33]. The intestinal flora is considered “the second brain” or “the second genome” of humans and is one of the most complex microbial communities, including more than 1000 bacteria, involved in the coding of more than 3 million nonredundant genes; moreover, its quantity is approximately equal to the total number of host human cells[9, 10]. The intestinal flora and the human body are interdependent, forming a state of dynamic balance that can change with changes in age, diet, environment, etc. Studies have demonstrated that the occurrence of type II diabetes, PCOS, and Alzheimer’s disease is associated with changes in the intestinal flora[34–37]. Other studies signified the discovery and characterization of the gut bacteria-generated compound TMAO and other gut bacteria-generated compounds that are negatively associated with multiple diseases, thus providing potential therapeutic goals that improve overall patient health[38–40]. Further research on the role of TMAO may provide new ideas for the diagnosis, monitoring and clinical treatment of related diseases.

5. Abbreviations

PCOS Polycystic ovary syndrome

TMAO Trimethylamine N-oxide

TMA Trimethylamine

IVM In vitro maturation

FINS. Fasting insulin

LH Luteinizing hormone

FSH Follicle-stimulating hormone

DMB 3,3-dimethyl-1-butanol

HA Hyperandrogenism

IR Insulin resistance

T2DM Type 2 diabetes mellitus

CVD Cardiovascular disease

AMH Anti-Müllerian hormone

IGF Insulin-like growth factor

FBG Fasting blood glucose

ELISA Enzyme-linked immunosorbent assay

PVDF Polyvinylidene fluoride

PMSG Pregnant mare serum gonadotropin

ΔΨm Mitochondrial membrane potential

SDHB Succinate dehydrogenase complex subunit B

HUVECs Human umbilical vein endothelial cells

Declarations

1) Ethics approval and consent to participate

All animal experiments were carried out in accordance with the principles and guidelines for the use of laboratory animals and approved by the Institutional Animal Care and Use Committee of Wuhan Union Hospital, Tongji medical college, HUST. Consent for publication

2) Availability of data and materials

The data generated during the current study are available from the corresponding author on reasonable request.

3) Competing interests

The authors declare that they have no competing interests.

4) Funding

This study was supported by the Natural Science Foundation of Hubei Province (Grant number 02.07.14040102). The funder played no role in the interpretation or writing of the manuscript in this study.

5) Authors' contributions

Huang Jiayu and Zhang Hanke analyzed data and wrote the paper. Huang Jiayu, Liu Jiaying, Guo Jing and Li Chong performed experiments. Qin Yinhua, Liu Jiaying and Guo Jing performed investigation, Yin Minuo edited the paper. Gao Ying and Li Jingyu conceived the study, reviewed and edited the paper. All authors read and approved the final version of the manuscript.

6) Acknowledgements

The authors thank the staff of the Department of Gynaecology and Obstetrics, Union Hospital, Tongji Medical College Huazhong University of Science and Technology and Chongqing Key Laboratory of Human Embryo Engineering, Chongqing Reproductive and Genetics Institute, Chongqing Health Center for Women and Children, Chongqing, China for their cooperation and their permission to conduct this study.

References

1. Escobar-Morreale, H.F., *Polycystic ovary syndrome: definition, aetiology, diagnosis and treatment.* Nat Rev Endocrinol, 2018. **14**(5): p. 270-284.
2. He, F.F. and Y.M. Li, *Role of gut microbiota in the development of insulin resistance and the mechanism underlying polycystic ovary syndrome: a review.* J Ovarian Res, 2020. **13**(1): p. 73.
3. Yildiz, B.O., et al., *Prevalence, phenotype and cardiometabolic risk of polycystic ovary syndrome under different diagnostic criteria.* Hum Reprod, 2012. **27**(10): p. 3067-73.

4. Gupta, M., et al., *Correlation of body mass index (BMI), anti-mullerian hormone (AMH), and insulin resistance among different polycystic ovary syndrome (PCOS) phenotypes - a cross-sectional study.* Gynecol Endocrinol, 2019: p. 1-4.
5. Rotterdam, E.A.-S.P.C.W.G., *Revised 2003 consensus on diagnostic criteria and long-term health risks related to polycystic ovary syndrome.* Fertil Steril, 2004. **81**(1): p. 19-25.
6. Shroff, R., et al., *Risk of metabolic complications in the new PCOS phenotypes based on the Rotterdam criteria.* Fertil Steril, 2007. **88**(5): p. 1389-95.
7. Peigne, M. and D. Dewailly, *Long term complications of polycystic ovary syndrome (PCOS).* Ann Endocrinol (Paris), 2014. **75**(4): p. 194-9.
8. Palomba, S., J. Daolio, and G.B. La Sala, *Oocyte Competence in Women with Polycystic Ovary Syndrome.* Trends Endocrinol Metab, 2017. **28**(3): p. 186-198.
9. Sender, R., S. Fuchs, and R. Milo, *Are We Really Vastly Outnumbered? Revisiting the Ratio of Bacterial to Host Cells in Humans.* Cell, 2016. **164**(3): p. 337-40.
10. Sender, R., S. Fuchs, and R. Milo, *Revised Estimates for the Number of Human and Bacteria Cells in the Body.* PLoS Biol, 2016. **14**(8): p. e1002533.
11. Zhang, D., et al., *Serum zonulin is elevated in women with polycystic ovary syndrome and correlates with insulin resistance and severity of anovulation.* Eur J Endocrinol, 2015. **172**(1): p. 29-36.
12. Qi, X., et al., *Gut microbiota-bile acid-interleukin-22 axis orchestrates polycystic ovary syndrome.* Nat Med, 2019.
13. Tremellen, K. and K. Pearce, *Dysbiosis of Gut Microbiota (DOGMA)--a novel theory for the development of Polycystic Ovarian Syndrome.* Med Hypotheses, 2012. **79**(1): p. 104-12.
14. Liu, R., et al., *Dysbiosis of Gut Microbiota Associated with Clinical Parameters in Polycystic Ovary Syndrome.* Front Microbiol, 2017. **8**: p. 324.
15. Schiattarella, G.G., et al., *Gut microbe-generated metabolite trimethylamine-N-oxide as cardiovascular risk biomarker: a systematic review and dose-response meta-analysis.* Eur Heart J, 2017. **38**(39): p. 2948-2956.
16. Zhu, W., et al., *Gut Microbial Metabolite TMAO Enhances Platelet Hyperreactivity and Thrombosis Risk.* Cell, 2016. **165**(1): p. 111-124.
17. Barrea, L., et al., *A New Light on Vitamin D in Obesity: A Novel Association with Trimethylamine-N-Oxide (TMAO).* Nutrients, 2019. **11**(6).
18. Rostamtabar, M., et al., *Elevated expression of IL-18 but not IL-1beta gene is associated with NALP3 and AIM2 inflammasome in Polycystic Ovary Syndrome.* Gene, 2020. **731**: p. 144352.
19. Wang, Z., et al., *Gut flora metabolism of phosphatidylcholine promotes cardiovascular disease.* Nature, 2011. **472**(7341): p. 57-63.
20. Koeth, R.A., et al., *Intestinal microbiota metabolism of L-carnitine, a nutrient in red meat, promotes atherosclerosis.* Nat Med, 2013. **19**(5): p. 576-85.

21. Li, X.S., et al., *Gut microbiota-dependent trimethylamine N-oxide in acute coronary syndromes: a prognostic marker for incident cardiovascular events beyond traditional risk factors.* Eur Heart J, 2017. **38**(11): p. 814-824.
22. Huang, J., et al., *PCOS without hyperandrogenism is associated with higher plasma Trimethylamine N-oxide levels.* BMC Endocr Disord, 2020. **20**(1): p. 3.
23. Nagy, R.A., et al., *Trimethylamine-N-oxide is present in human follicular fluid and is a negative predictor of embryo quality.* Hum Reprod, 2020. **35**(1): p. 81-88.
24. Poretsky, L., J. Clemons, and K. Bogovich, *Hyperinsulinemia and human chorionic gonadotropin synergistically promote the growth of ovarian follicular cysts in rats.* Metabolism, 1992. **41**(8): p. 903-10.
25. Zhang, Y., et al., *Molecular characterization of insulin resistance and glycolytic metabolism in the rat uterus.* Sci Rep, 2016. **6**: p. 30679.
26. Zhang, Y., et al., *Metformin Ameliorates Uterine Defects in a Rat Model of Polycystic Ovary Syndrome.* EBioMedicine, 2017. **18**: p. 157-170.
27. Li, T., et al., *Increased circulating trimethylamine N-oxide contributes to endothelial dysfunction in a rat model of chronic kidney disease.* Biochem Biophys Res Commun, 2018. **495**(2): p. 2071-2077.
28. Patti, M.E. and S. Corvera, *The role of mitochondria in the pathogenesis of type 2 diabetes.* Endocr Rev, 2010. **31**(3): p. 364-95.
29. Hesselink, M.K., V. Schrauwen-Hinderling, and P. Schrauwen, *Skeletal muscle mitochondria as a target to prevent or treat type 2 diabetes mellitus.* Nat Rev Endocrinol, 2016. **12**(11): p. 633-645.
30. Arruda, A.P., et al., *Chronic enrichment of hepatic endoplasmic reticulum-mitochondria contact leads to mitochondrial dysfunction in obesity.* Nat Med, 2014. **20**(12): p. 1427-35.
31. Wu, P., et al., *Trimethylamine N-oxide promotes apoE(-/-) mice atherosclerosis by inducing vascular endothelial cell pyroptosis via the SDHB/ROS pathway.* J Cell Physiol, 2020.
32. Shukla, P. and S. Mukherjee, *Mitochondrial dysfunction: An emerging link in the pathophysiology of polycystic ovary syndrome.* Mitochondrion, 2020. **52**: p. 24-39.
33. Lozupone, C.A., et al., *, stability and resilience of the human gut microbiota.* Nature, 2012. **489**(7415): p. 220-30.
34. Szalkai, B. and V. Grolmusz, *Nucleotide 9-mers characterize the type II diabetic gut metagenome.* Genomics, 2016. **107**(4): p. 120-3.
35. Yurtdas, G. and Y. Akdevelioglu, *A New Approach to Polycystic Ovary Syndrome: The Gut Microbiota.* J Am Coll Nutr, 2019: p. 1-12.
36. Fung, T.C., C.A. Olson, and E.Y. Hsiao, *Interactions between the microbiota, immune and nervous systems in health and disease.* Nat Neurosci, 2017. **20**(2): p. 145-155.
37. Kim, M.S., et al., *Transfer of a healthy microbiota reduces amyloid and tau pathology in an Alzheimer's disease animal model.* Gut, 2019.

38. Lopez de Felipe, F., B. de Las Rivas, and R. Munoz, *Bioactive compounds produced by gut microbial tannase: implications for colorectal cancer development.* Front Microbiol, 2014. **5**: p. 684.
39. Heaney, L.M., *Applying mass spectrometry-based assays to explore gut microbial metabolism and associations with disease.* Clin Chem Lab Med, 2019.
40. Qi, J., et al., *Alternating consumption of beta-glucan and quercetin reduces mortality in mice with colorectal cancer.* Food Sci Nutr, 2019. **7**(10): p. 3273-3285.

Figures

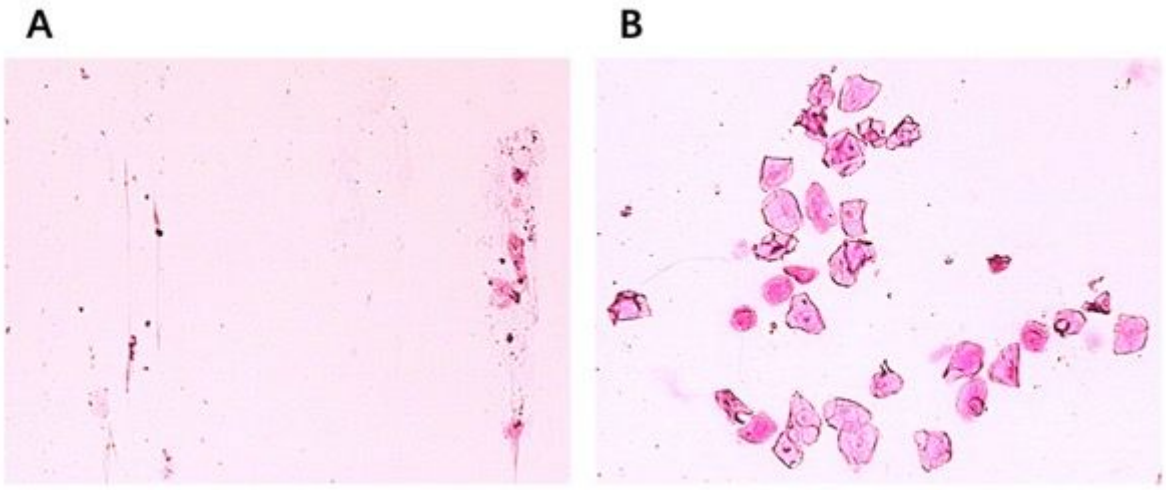

Figure 1

Vaginal smears of rats in the DMB group (A) rats with disordered estrus cycle; (B) some rats still have normal estrous cycles

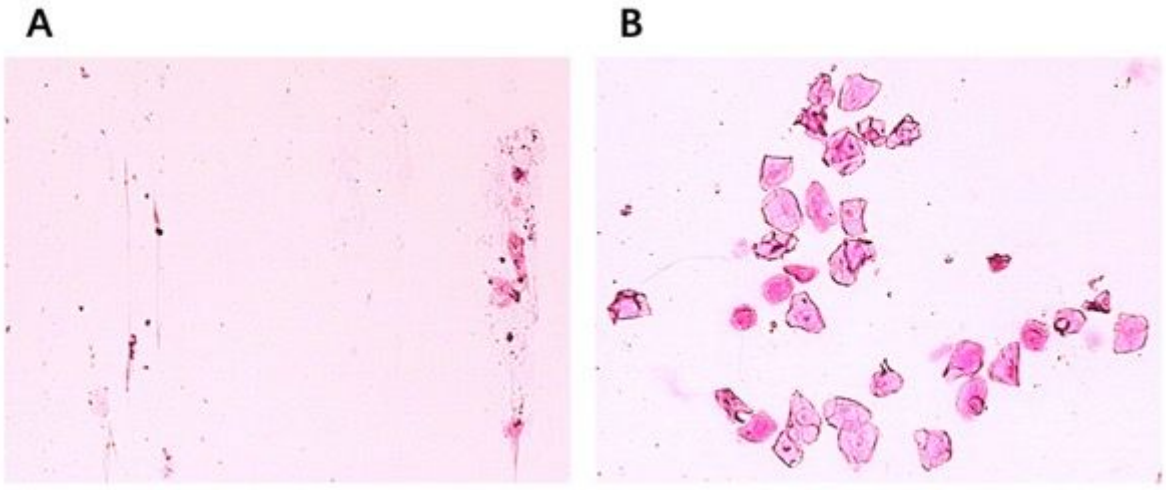

Figure 1

Vaginal smears of rats in the DMB group (A) rats with disordered estrus cycle; (B) some rats still have normal estrous cycles

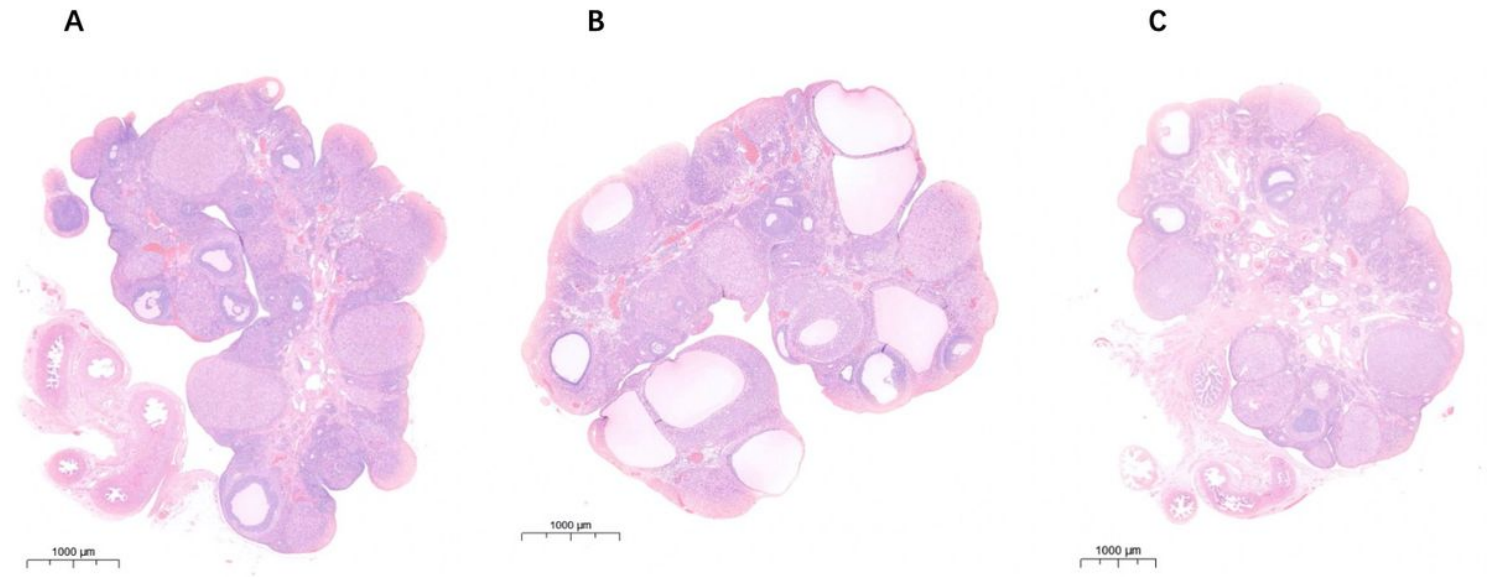

Figure 2

HE staining of rat ovaries from the (A) control group, (B) PCOS group, (C) DMB group

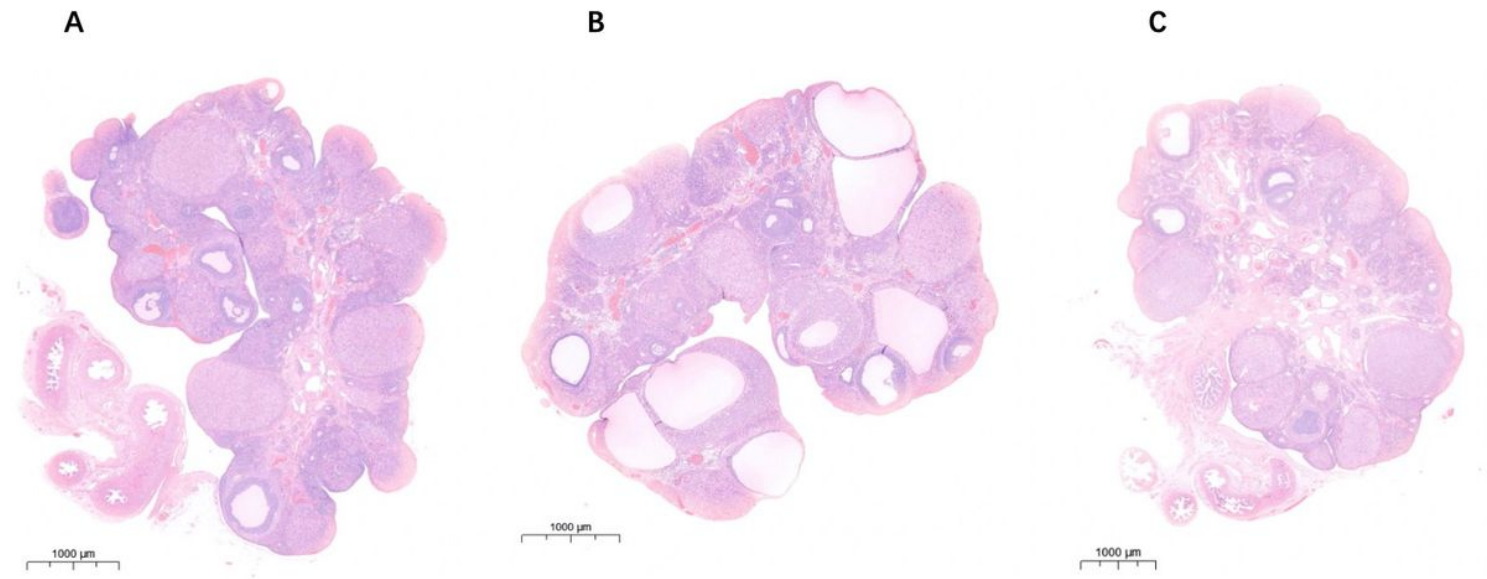

Figure 2

HE staining of rat ovaries from the (A) control group, (B) PCOS group, (C) DMB group

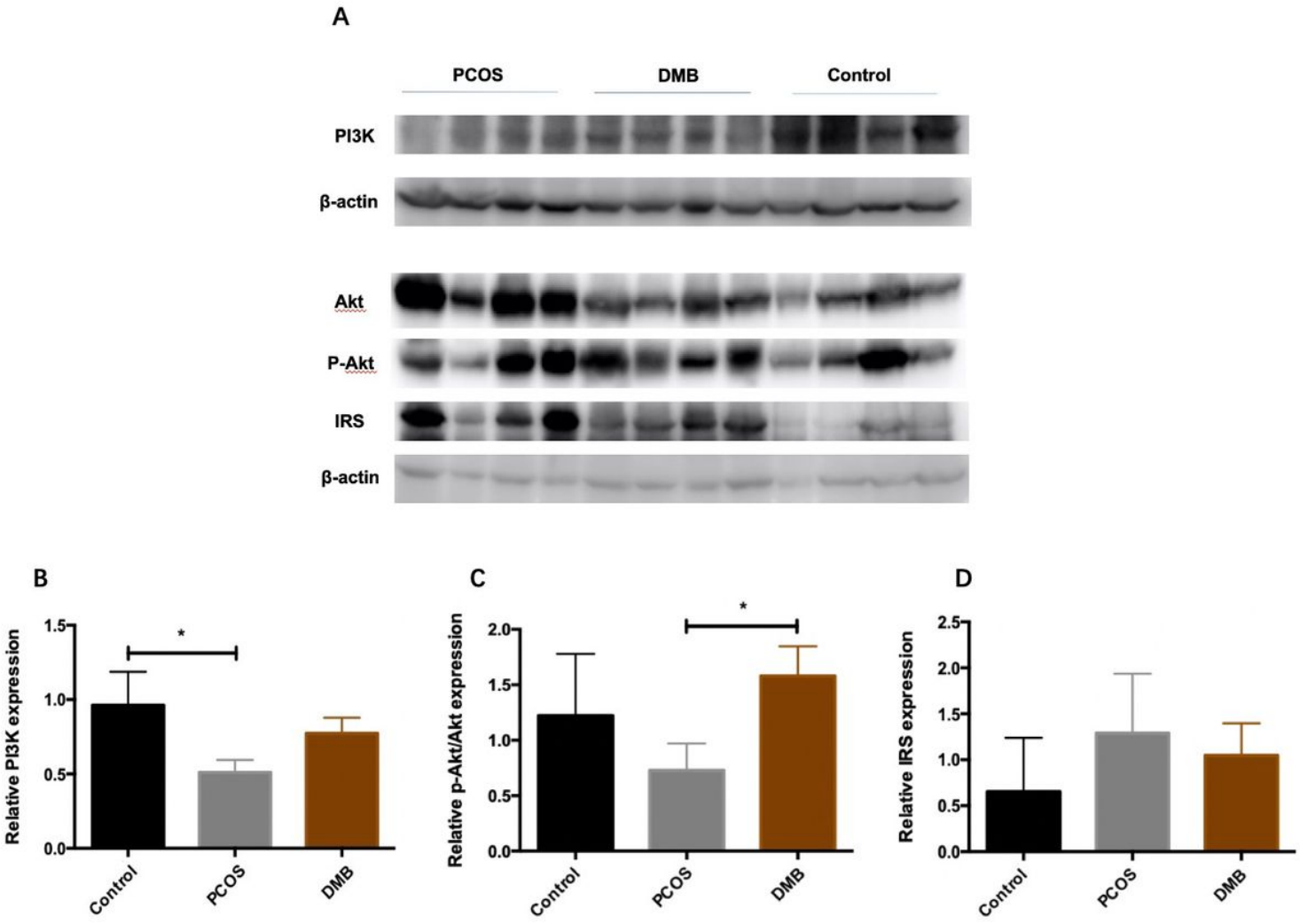

Figure 3

(A) Western blot analysis was performed to detect the protein expression levels of PI3K, Akt, p-Akt, and IRS in different groups of rats; (B-D) analysis of the results corresponding to those shown in (A); the results were normalized to the internal reference, β-actin; *P < 0.05

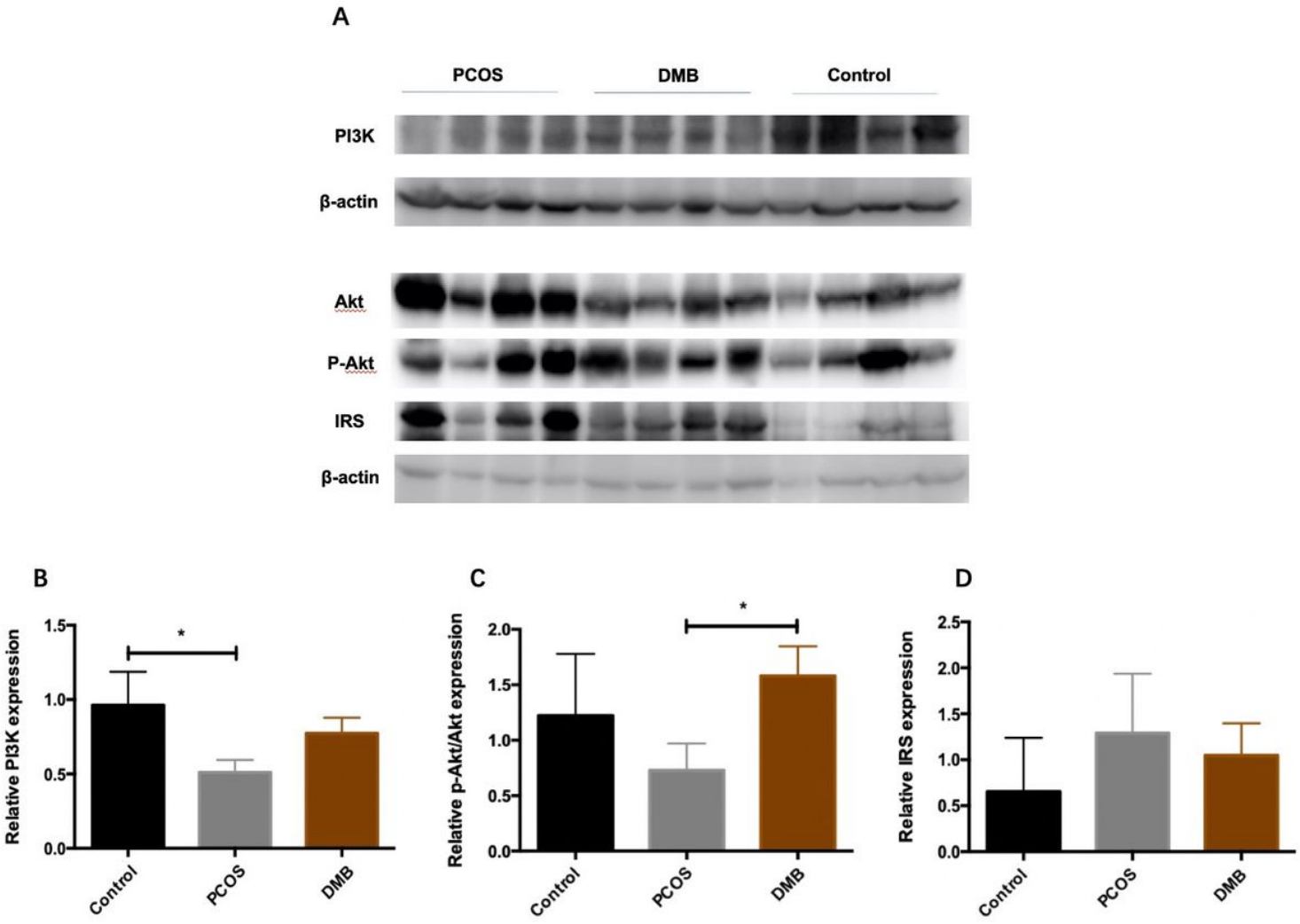

Figure 3

(A) Western blot analysis was performed to detect the protein expression levels of PI3K, Akt, p-Akt, and IRS in different groups of rats; (B-D) analysis of the results corresponding to those shown in (A); the results were normalized to the internal reference, β-actin; *P < 0.05

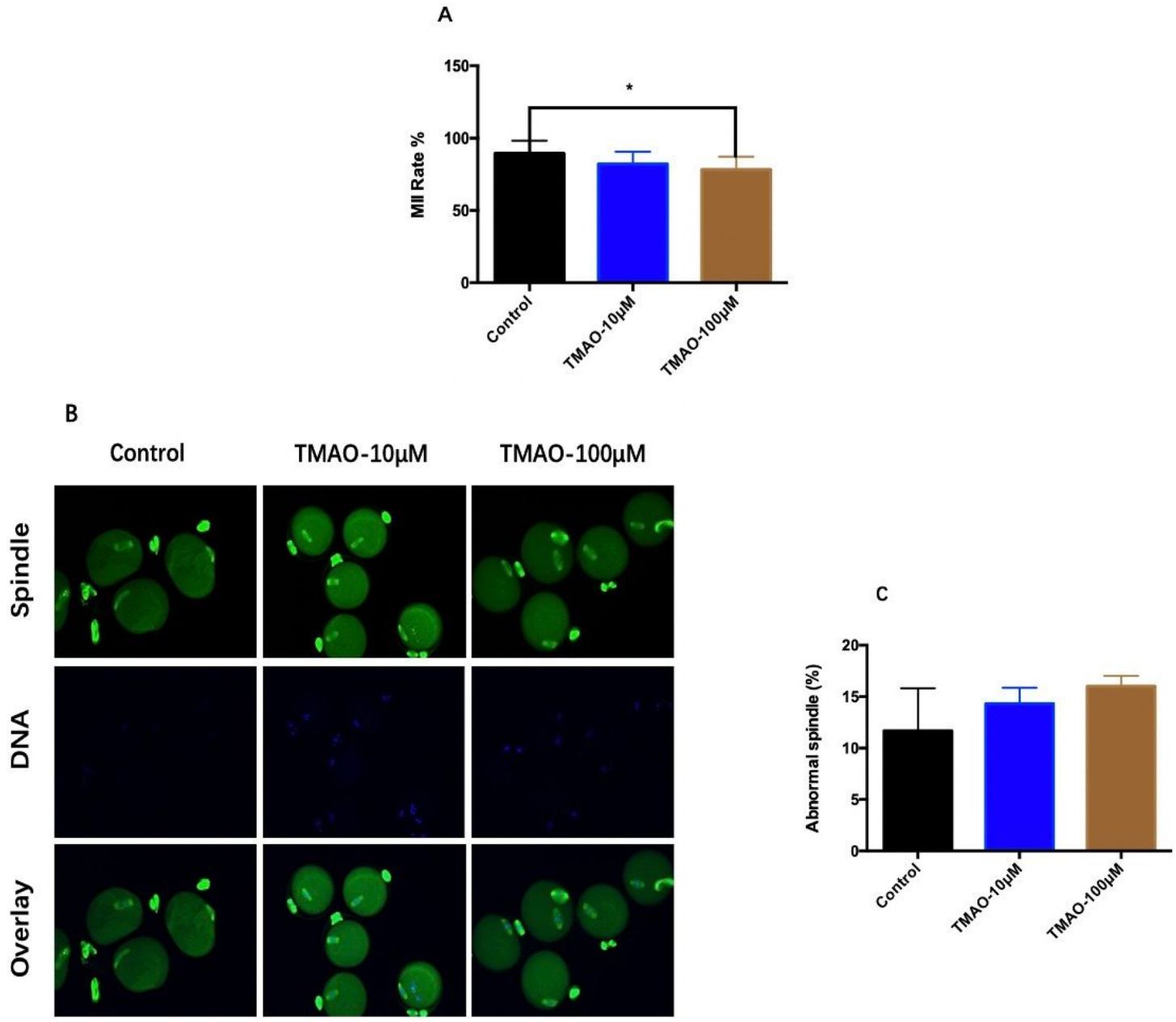

Figure 4

(A) Difference in the MII rate among different TMAO concentration groups and the control group; *P<0.05; (B) the morphology and structure of the spindles treated with TMAO were not significantly different from the untreated spindles; (C) the spindle abnormality rate was not significantly different between the three groups

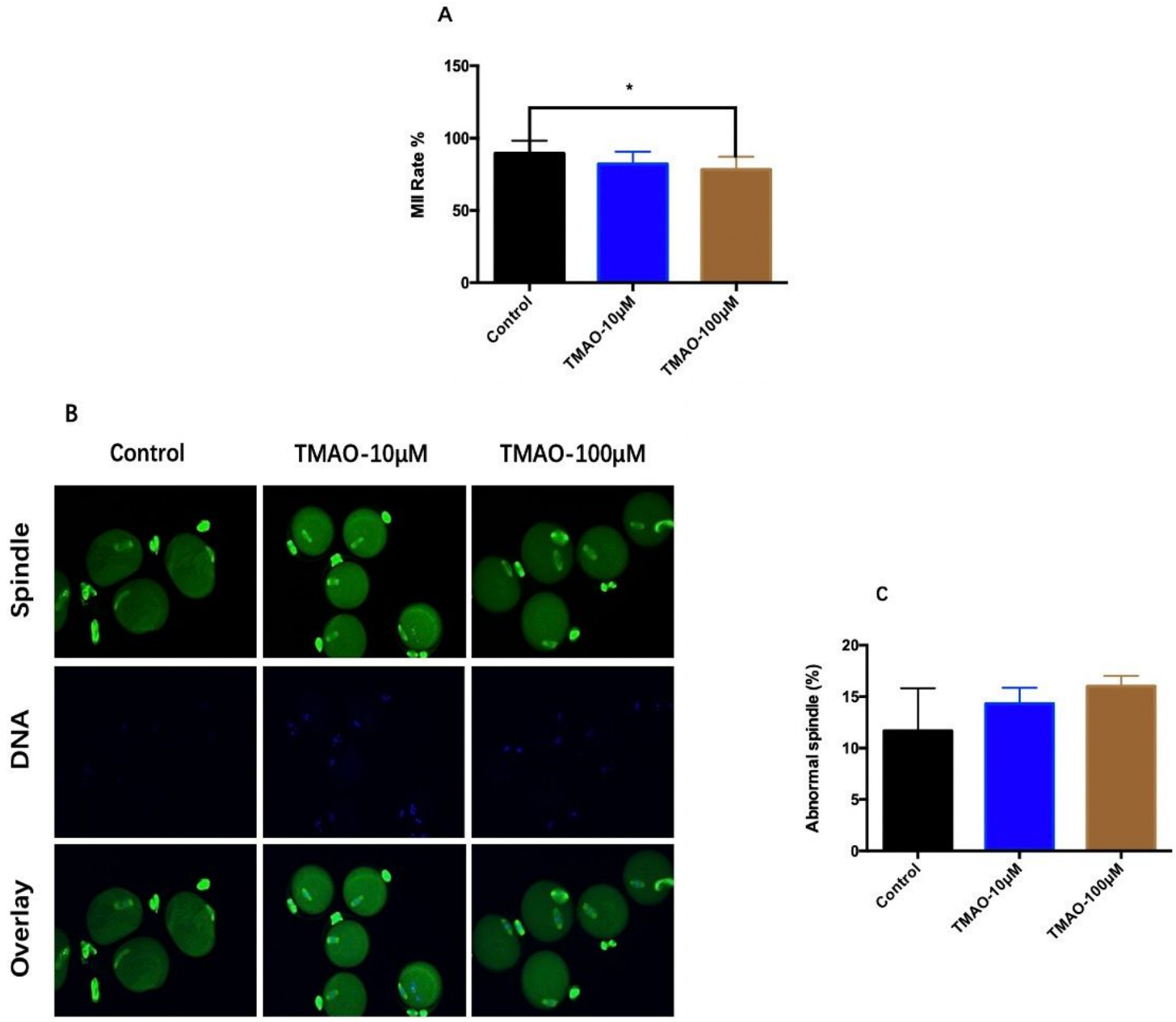

Figure 4

(A) Difference in the MII rate among different TMAO concentration groups and the control group; *P<0.05; (B) the morphology and structure of the spindles treated with TMAO were not significantly different from the untreated spindles; (C) the spindle abnormality rate was not significantly different between the three groups

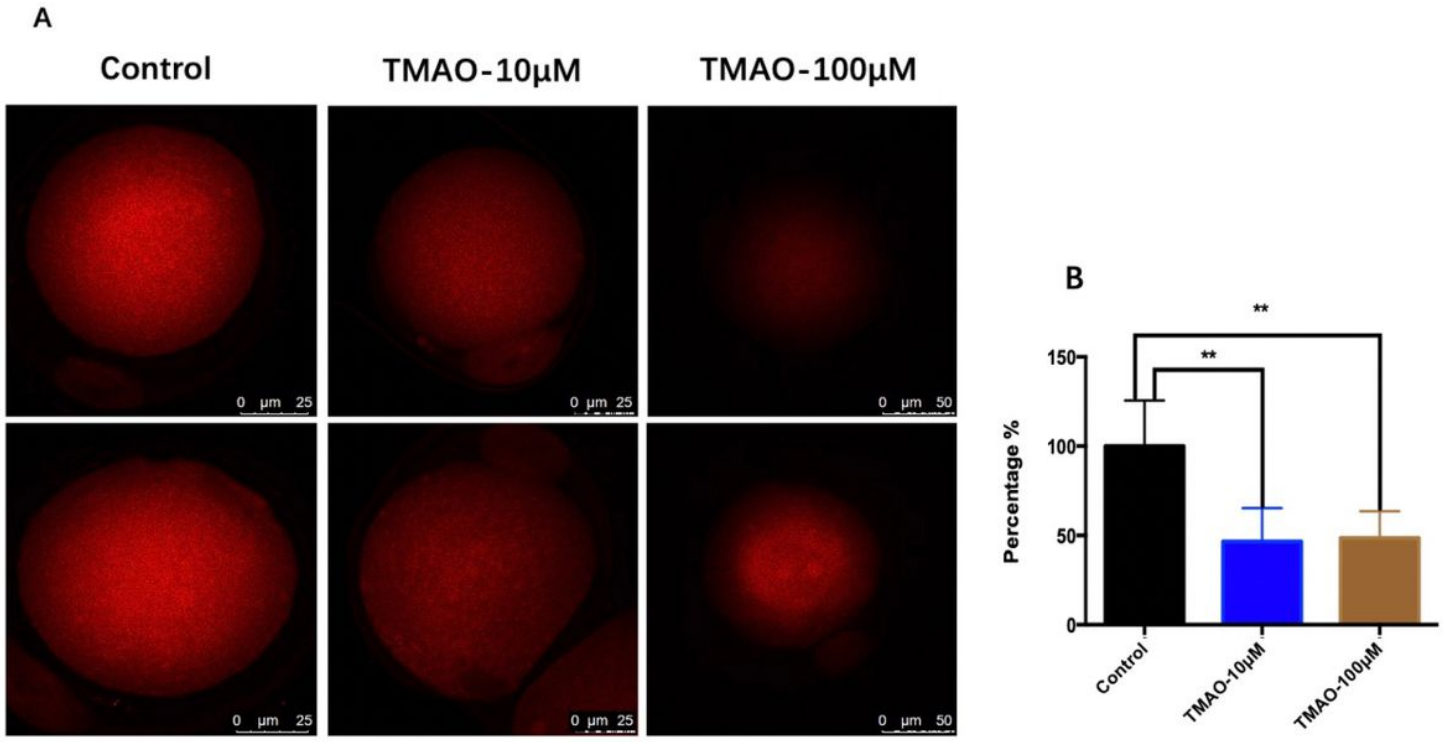

Figure 5

The effect of TMAO on the content and distribution of mitochondria in oocytes; (A) The mitochondria of oocytes in the control group are evenly distributed, whereas the fluorescence intensity of oocytes in the TMAO-10 μM and TMAO-100 μM experimental groups is weakened, and the mitochondria appear aggregated and distributed; (B) Relative fluorescence intensity of oocyte mitochondria, ****P< 0.0001

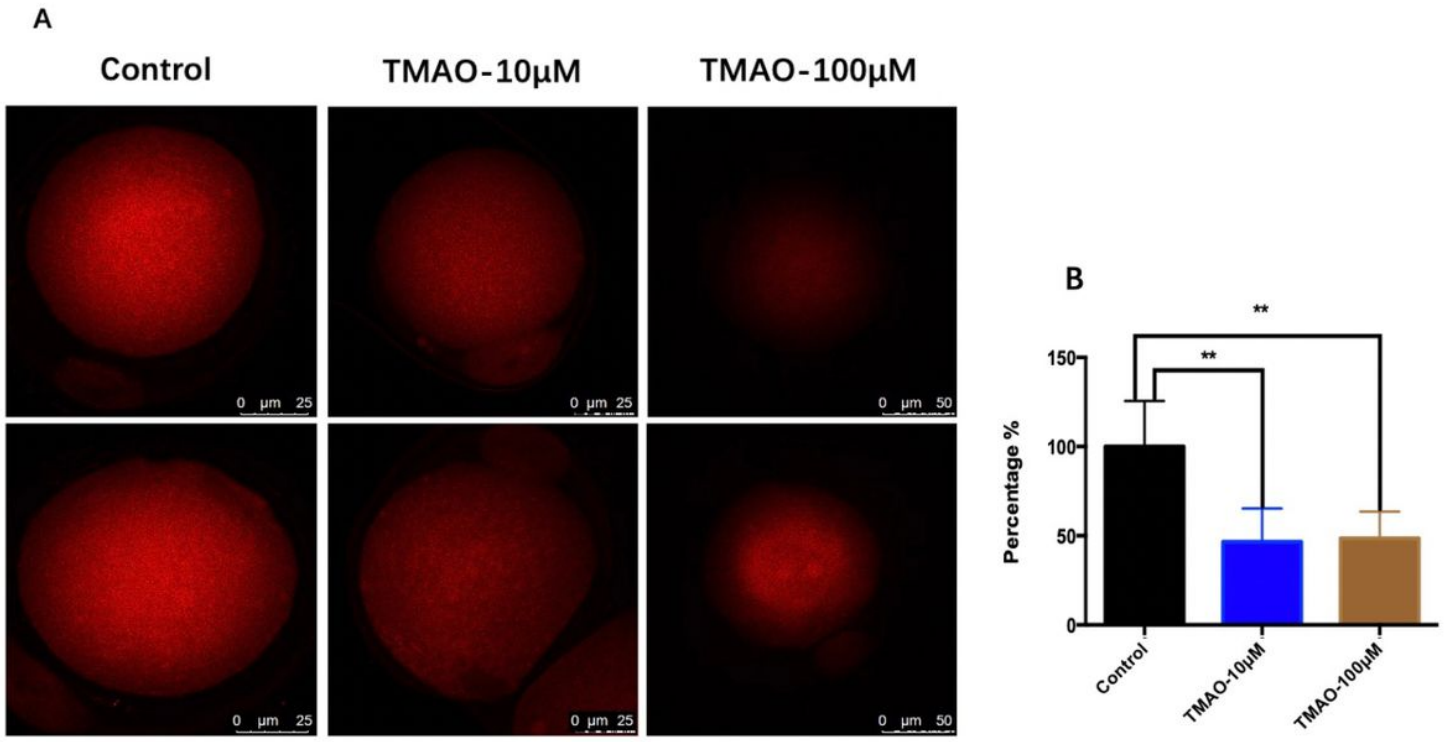

Figure 5

The effect of TMAO on the content and distribution of mitochondria in oocytes; (A) The mitochondria of oocytes in the control group are evenly distributed, whereas the fluorescence intensity of oocytes in the TMAO-10 μM and TMAO-100 μM experimental groups is weakened, and the mitochondria appear aggregated and distributed; (B) Relative fluorescence intensity of oocyte mitochondria, ****P< 0.0001

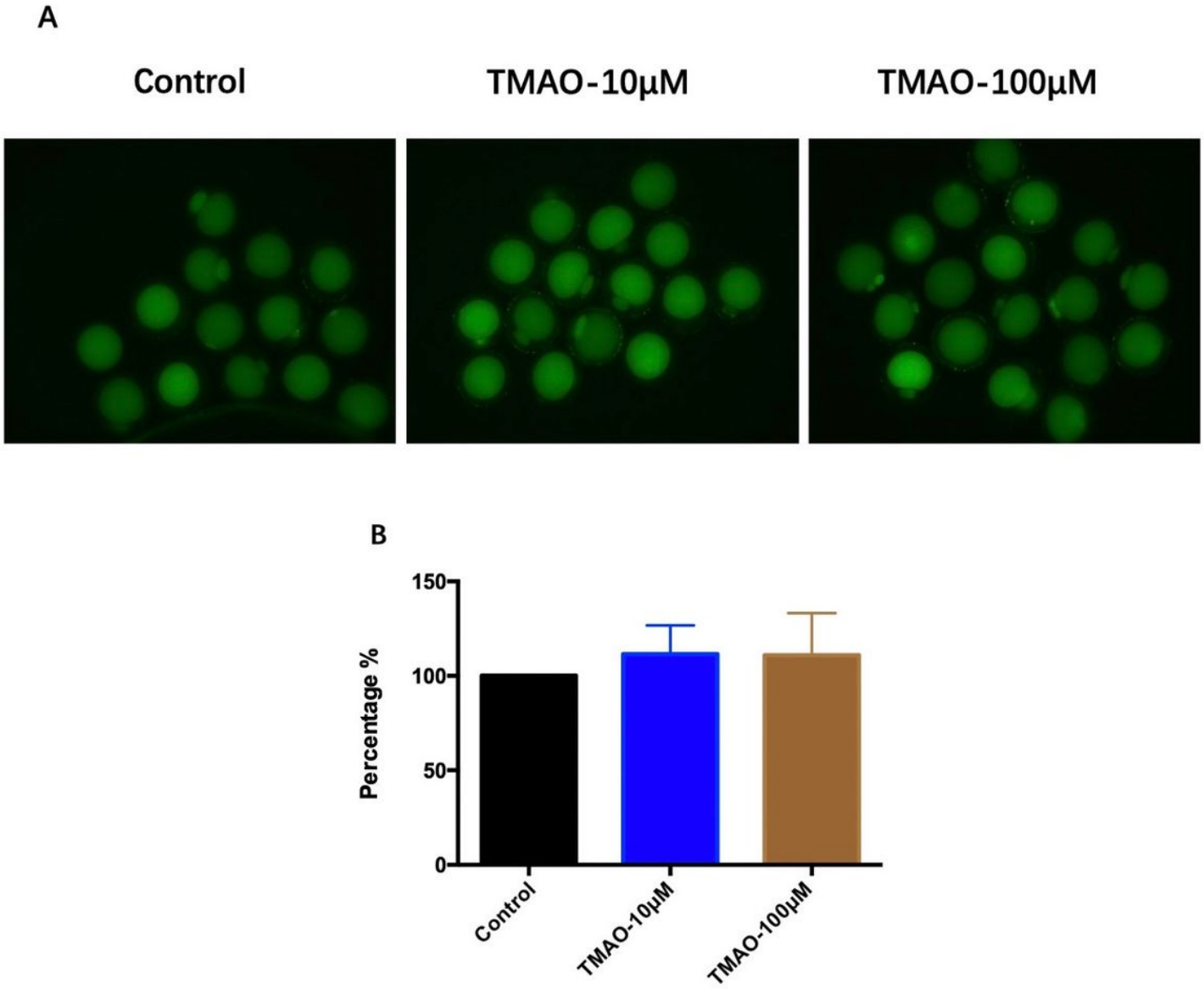

Figure 6

The effect of TMAO on ROS accumulation in oocytes; (A) the content of ROS was not significantly different between groups; (B) the relative intensity of ROS fluorescence in each group

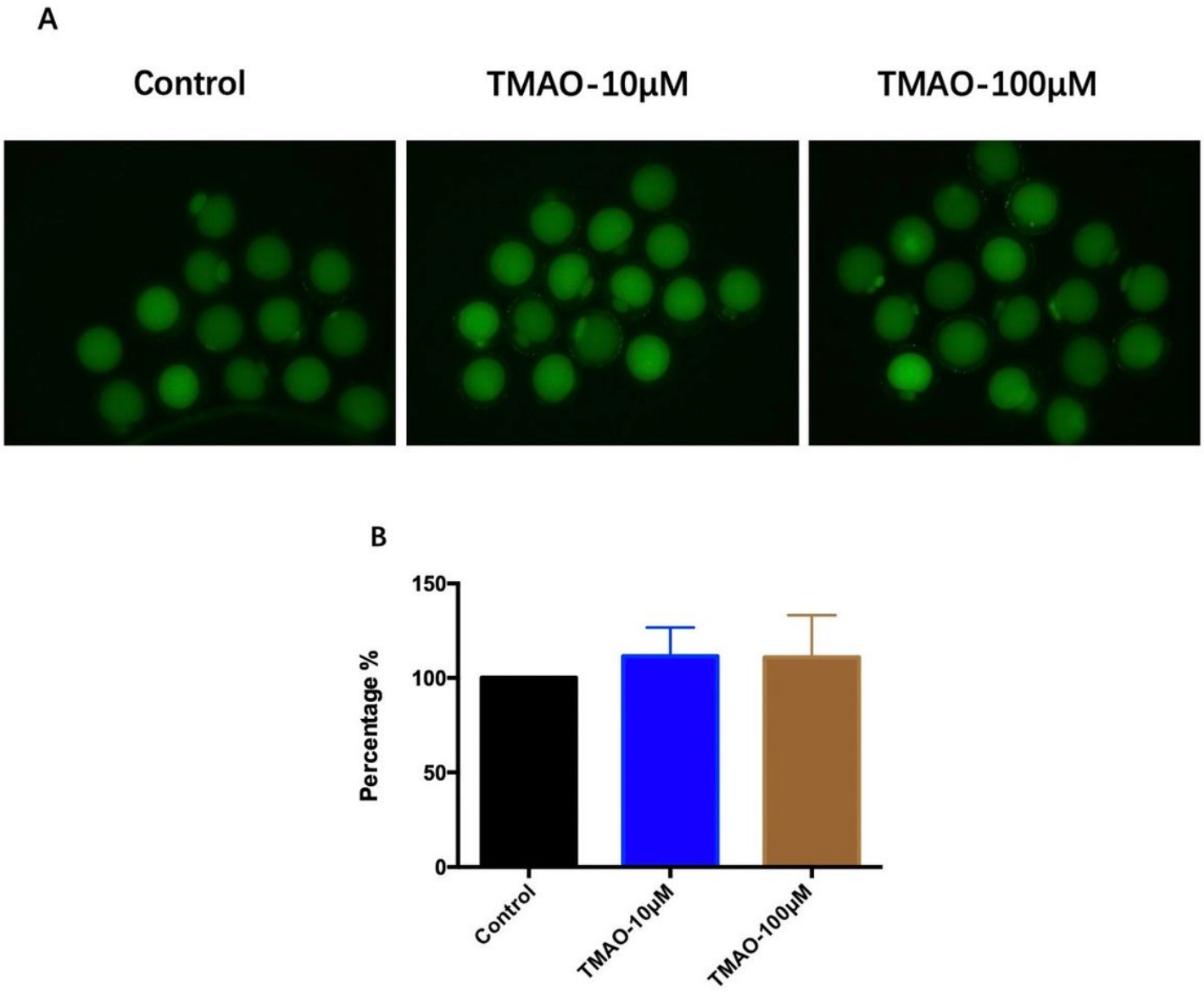

Figure 6

The effect of TMAO on ROS accumulation in oocytes; (A) the content of ROS was not significantly different between groups; (B) the relative intensity of ROS fluorescence in each group

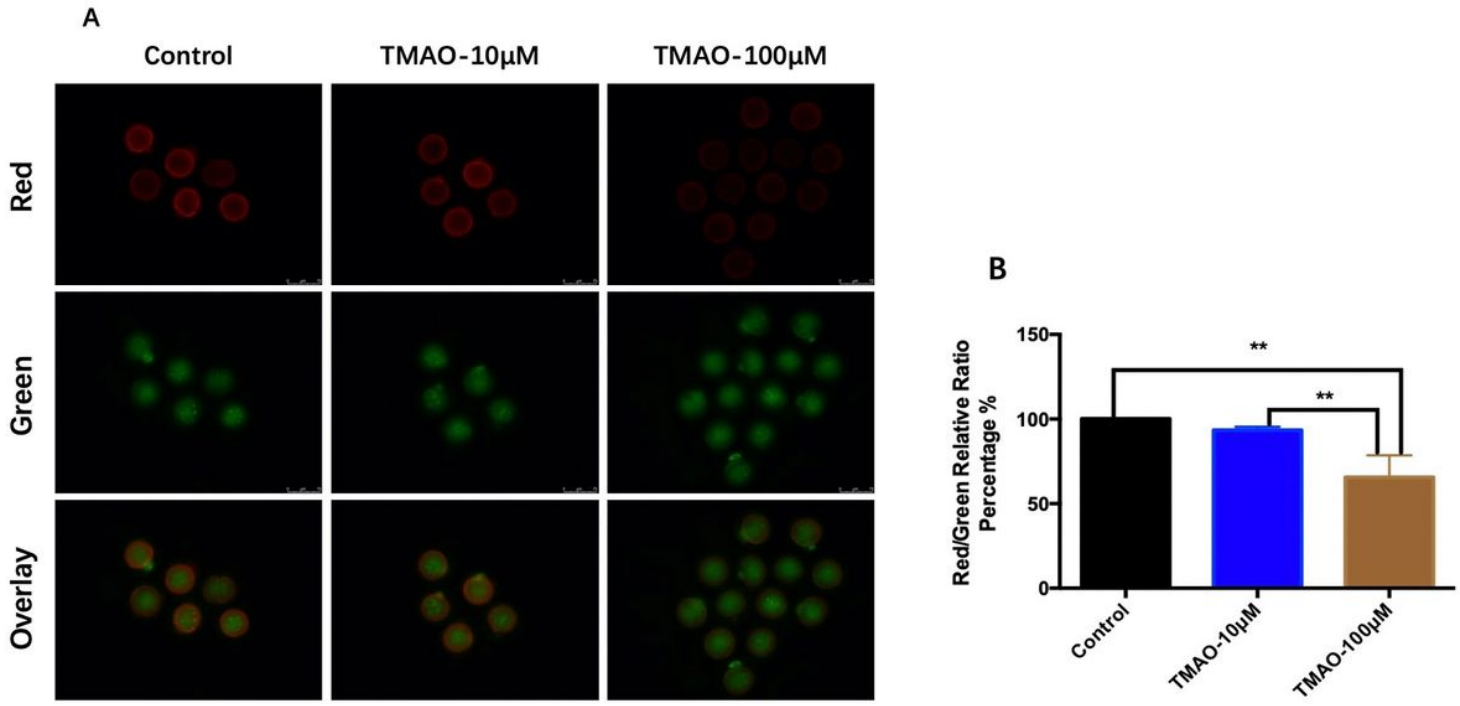

Figure 7

The effect of TMAO on the mitochondrial membrane potential of oocytes; (A) the mitochondrial membrane potential of mouse oocytes; the average ratio of red-green fluorescence in the TMAO-100 μM group was significantly reduced; (B) the mitochondrial membrane potential decreased significantly in the TMAO-100 μM group; **P<0.01

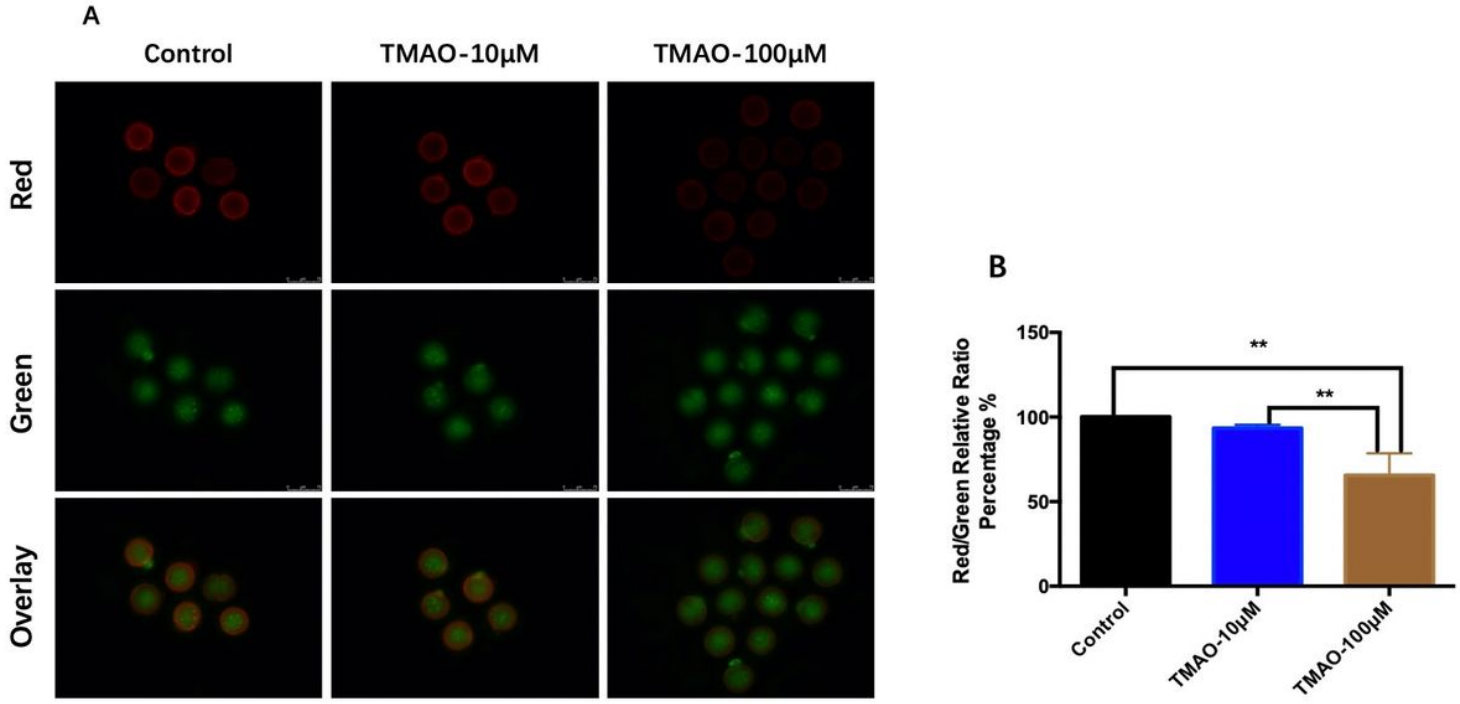

Figure 7

The effect of TMAO on the mitochondrial membrane potential of oocytes; (A) the mitochondrial membrane potential of mouse oocytes; the average ratio of red-green fluorescence in the TMAO-100 μM group was significantly reduced; (B) the mitochondrial membrane potential decreased significantly in the TMAO-100 μM group; **P<0.01

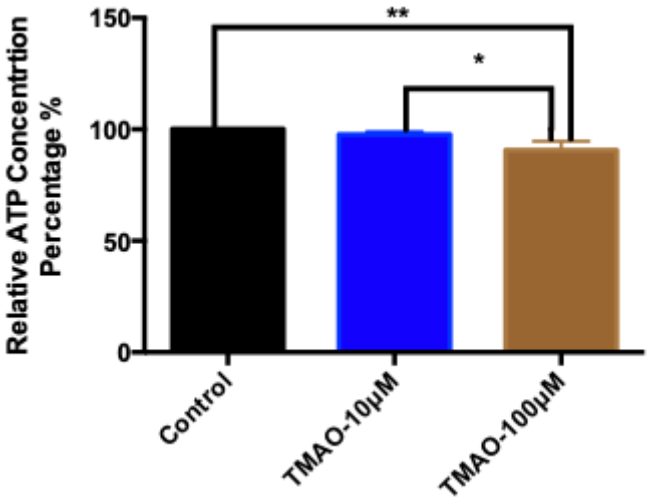

Figure 8

The effect of TMAO on ATP production in oocytes; the ATP content of oocytes in the TMAO-100 μM group was lower than that of oocytes in the control and TMAO-10 μM groups; **P<0.01, *P<0.05

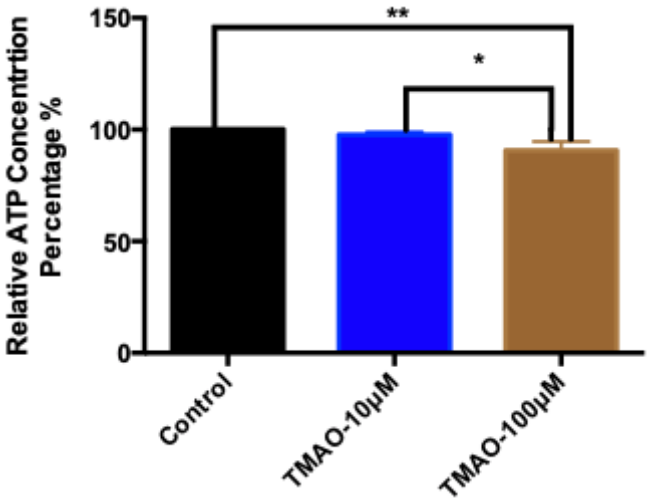

Figure 8

The effect of TMAO on ATP production in oocytes; the ATP content of oocytes in the TMAO-100 μM group was lower than that of oocytes in the control and TMAO-10 μM groups; **P<0.01, *P<0.05

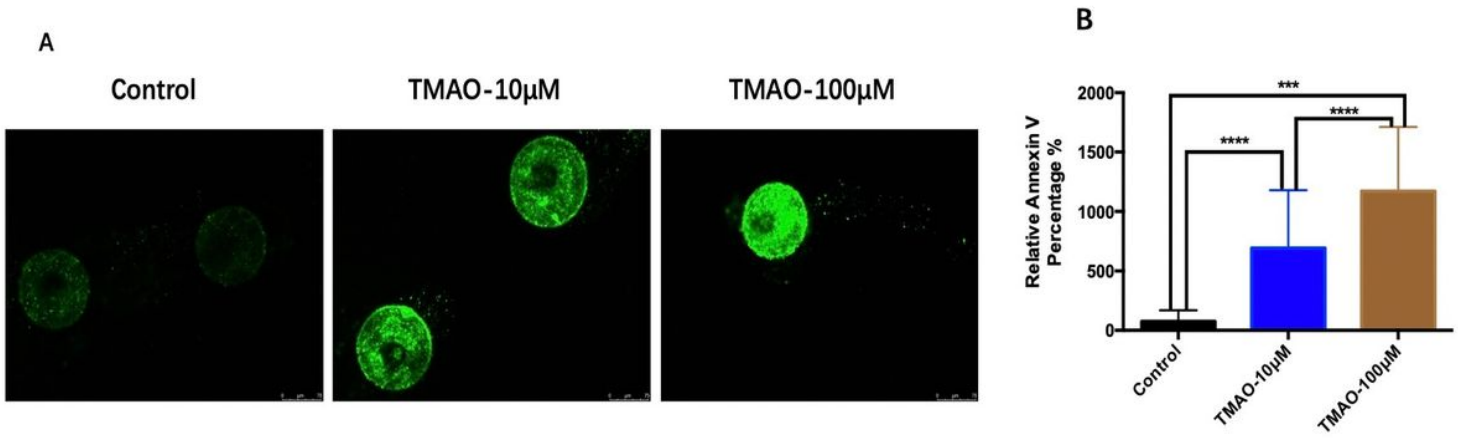

Figure 9

The effect of TMAO on the early apoptosis of mouse oocytes; (A) the rate of early apoptosis in oocytes from the control group was very low, and the rate of early apoptosis in oocytes from the TMAO groups was high; the higher the concentration was, the higher the degree of apoptosis; (B) oocyte apoptosis was significantly increased in the TMAO-100 μM group; ****P< 0.0001, ***P< 0.001

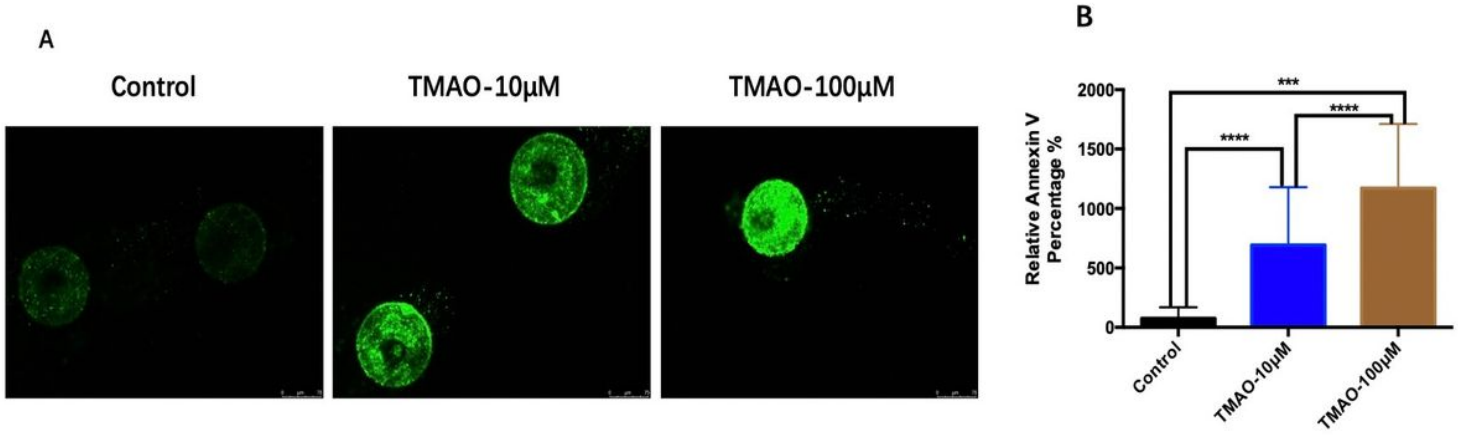

Figure 9

The effect of TMAO on the early apoptosis of mouse oocytes; (A) the rate of early apoptosis in oocytes from the control group was very low, and the rate of early apoptosis in oocytes from the TMAO groups was high; the higher the concentration was, the higher the degree of apoptosis; (B) oocyte apoptosis was significantly increased in the TMAO-100 μM group; ****P< 0.0001, ***P< 0.001